

Membrane Association and Contact Formation by a Synthetic Analogue of Polymyxin B and Its Fluorescent Derivatives

Adrià Clausell,[†] Francesc Rabanal,[‡] Maria Garcia-Subirats,[‡] M. Asunción Alsina,[†] and Yolanda Cajal^{*,†}

Physical Chemistry Department, Faculty of Pharmacy, University of Barcelona, Avn. Joan XXIII s/n, 08028 Barcelona, Spain, and Department of Organic Chemistry, University of Barcelona, Martí i Franquès 1, 08028 Barcelona, Spain

Received: September 14, 2005; In Final Form: December 23, 2005

sP-B is a synthetic analogue of the natural lipopeptide antibiotic polymyxin B (PxB) that maintains the ability of the parent compound to form vesicle–vesicle contacts and induce lipid exchange. Exchange is selective, and only monoanionic phospholipids such as 1-palmitoyl-2-oleoyl-glycero-*sn*-3-phosphoglycerol (POPG) are transferred, whereas dianionic phospholipids such as 1-palmitoyl-2-oleoyl-glycero-*sn*-3-phosphate (POPA) are not, as shown by fluorescence experiments based on the excimer/monomer ratio of pyrene-labeled phospholipids. Synthetic fluorescent analogues of sP-B are used to investigate the peptide position and orientation in the intermembrane contacts: sP-Bw, an analogue that contains D-tryptophan (D-Trp) instead of the naturally occurring D-phenylalanine, and sP-Bpy, incorporating a pyrene group at the N-terminus. Tryptophan fluorescence, anisotropy, and quenching measurements performed with sP-Bw indicate that the peptide binds and inserts in anionic vesicles of POPG and POPA. However, significant differences are seen depending on the lipid composition, as also demonstrated by fluorescence resonance energy transfer (FRET) experiments from Trp to 7-nitro-2-1,3-benzoxadiazol (NBD) groups at the interface. Intermolecular FRET using sP-Bw as the donor and sP-Bpy as the acceptor indicates self-association of the peptide, possibly forming dimers, when bound to POPG vesicles at concentrations that induce the vesicle–vesicle contacts.

Introduction

Antibiotic resistance is a growing concern due to the extensive use of classical antibiotics. The continuous emergence of bacterial strains that are resistant to conventional antibiotics has led to intensive efforts aimed at the development of new drugs that do not generate bacterial resistance.¹ In this context, antimicrobial peptides (AMPs) are considered to have a great potential to become a new class of antibiotics to treat antibiotic-resistant bacterial infections and septic shock.^{2,3} More than 880 different AMPs have already been identified or predicted from nucleic acid sequences.⁴ They are a unique and diverse group of molecules produced by a variety of invertebrate, plant, and animal species, and despite their diversity in structure, most of them share common trends, such as an amphipathic character and several cationic residues, which allows them to interact strongly with the anionic bacterial membranes and ultimately kill the bacteria by different mechanisms related to the alteration of the membrane.

Polymyxin B (PxB) is a naturally occurring cyclic antibiotic lipopeptide that is very potent and selective against Gram-negative microorganisms. Resistance to polymyxin is very uncommon^{5,6} and generally due to reversible adaptation through a change in the bacterium's outer membrane, preventing the drug from binding the lipopolysaccharide, a necessary first step in the mechanism of antimicrobial action.⁷ In addition, PxB is the most efficient agent for the treatment of septic shock, due to its high efficient binding and detoxification of lipid A. Despite

these advantages, since their discovery in 1947, polymyxins have had very limited clinical use due to their nephrotoxicity. However, more recent studies reveal that the use of PxB to treat multiresistant Gram-negative infections is highly effective and associated with a lower rate of toxicity than previously described, reportedly due to the high concentrations of drug used in the initial experiments.^{8,9} The mechanism of action of PxB is not based on a detergent or lytic effect on the membrane, as was previously thought. Biophysical studies using model membranes have demonstrated that, at the concentrations around the minimal inhibitory concentration (MIC), PxB induces the apposition of anionic vesicles and the formation of functional vesicle–vesicle contacts that support a fast and selective exchange of phospholipids exclusively between the outer monolayers of the vesicles in contact, maintaining intact the inner monolayers and the aqueous contents.^{10–12} This biophysical phenomenon has been proposed as the mechanism of antibacterial action of PxB and several other antibiotic peptides.¹³ The discovery of new agents with a related antibacterial mode of action may generate antibiotics with minimal potential for selection of resistance and better therapeutical indexes. We have designed a series of synthetic peptides that mimic the primary and secondary structure of PxB, and we have determined their ability to form vesicle–vesicle contacts and induce phospholipid flow, adopting some of the remarkably sensitive methods based on fluorescence that have been developed during the past decade for detection of bilayer apposition, mixing, and fusion. The PxB synthetic analogue sP-B (see structure in Figure 1) maintains the major putative structural requirements for PxB activity: a cycle of seven amino acids with three positive charges due to L- α , γ -diaminobutyric acid (Dab) and the

* Corresponding author. Phone: 34-93-4035988. Fax: 34-93-4035987. E-mail: ycajal@ub.edu.

[†] Physical Chemistry Department, Faculty of Pharmacy.

[‡] Department of Organic Chemistry.

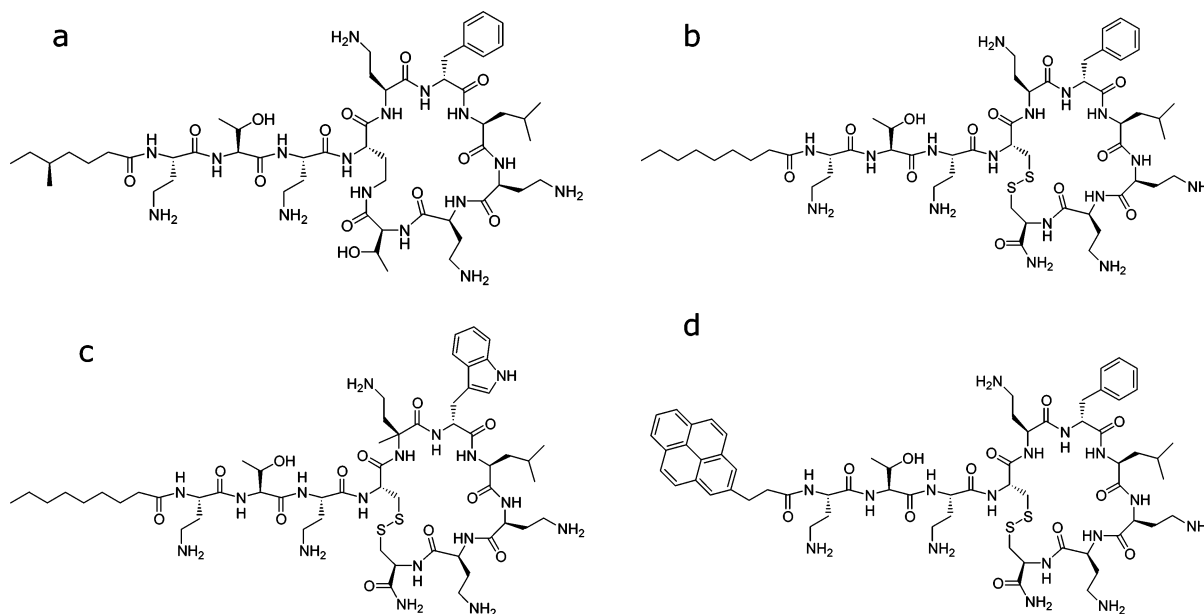


Figure 1. Sequences of PxB (a) and the synthetic analogues sP-B (b), sP-Bw (c), and sP-Bpy (d).

hydrophobic domain (D)-Phe-Leu, a linear tripeptide with two positive charges also due to Dab, and a middle length hydrophobic N-terminal chain. We have already shown that sP-B forms functional vesicle-vesicle contacts and induces selective lipid exchange,¹⁴ as previously described for PxB. In this paper, we use spectroscopic methods to further characterize the interaction of sP-B with phospholipid membranes and the formation of vesicle-vesicle molecular contacts. For this purpose, two synthetic analogues of sP-B with intrinsic fluorescence, sP-Bw and sP-Bpy, have been synthesized (see structure in Figure 1). Analogue sP-Bw contains a tryptophan residue (D-Trp) instead of the D-Phe of sP-B, and analogue sP-Bpy is selectively labeled on the N-terminus with a pyrene-butanoate chain instead of the nonanoate chain present in the parent compound sP-B. The inclusion of D-Trp is very useful to characterize binding of the peptide to the membrane by fluorescence techniques. sP-Bw also serves as a donor for intermolecular resonance energy transfer (FRET) experiments with sP-Bpy used as the acceptor. FRET experiments are consistent with self-association of sP-B bound to anionic vesicles at the concentrations that induce the vesicle-vesicle contacts.

Experimental Section

Chemicals. Polymyxin B sulfate salt (PxB) and Trizma base (Tris) were purchased from Sigma-Aldrich (St Louis, MO). 1-Palmitoyl-2-oleoyl-glycero-*sn*-3-phosphatidic acid (POPA) and 1-palmitoyl-2-oleoyl-glycero-*sn*-3-phosphoglycerol (POPG) are from Avanti Polar Lipids (Alabaster, AL). Fluorescently labeled phospholipids—*N*-(7-nitro-2-1,3-benzoxadiazol-4-yl)-dioleoylphosphatidylethanolamine (NBD-PE), *N*-(lissamine rhodamine B sulfonyl)-dioleoyl phosphatidylethanolamine (Rh-PE), 1-hexadecanoyl-2-(1-pyrenedecanoyl) glycerol-*sn*-3-phosphoglycerol (pyPG), and 1-hexadecanoyl-2-(1-pyrenedecanoyl) glycerol-*sn*-3-phosphate (pyPA)—were purchased from Molecular Probes (Eugene, OR); the last one was obtained by custom-made synthesis. *N*-Fluorenylmethoxycarbonyl (Fmoc)-protected amino acids, namely, Fmoc-Dab(Boc)-OH, Fmoc-Cys(Trt)-OH, Fmoc-Thr(Bu)-OH, Fmoc-D-Phe-OH, Fmoc-D-Trp-OH, and Fmoc-Leu-OH, were purchased from Bachem (Bubendorf, Switzerland) and Fluka (Buchs, Switzerland). The chemical reagents *N,N*-diisopropylcarbodiimide (DIPCDI), *N*-

hydroxybenzotriazole (HOBt), trifluoroacetic acid (TFA) (Bio-Chemika quality) as well as nonanoic acid were also from Fluka (Buchs, Switzerland). Rink amide resin was purchased from Novabiochem (Läufelfingen, Switzerland).

Peptide Synthesis and Purification. Peptide synthesis was performed manually following standard Fmoc/^tBu procedures using DIPCDI/HOBt activation on a Rink amide resin.¹⁵ Once the sequence was assembled, cleavage of the peptides from the resin was carried out by acidolysis with TFA/triisopropylsilane/water (95:3:2, v/v) for 90 min. TFA was removed with a N₂ stream, and the oily residue was treated with dry diethyl ether to obtain the peptide precipitate. The solid peptide was isolated by centrifugation. This process was repeated three times. The homogeneity of peptide crudes was assessed by analytical high pressure liquid chromatography (HPLC) using Nucleosil C18 reverse phase columns (4 × 250 mm, 5 μm particle diameter and 120 Å pore size). Elution was carried out at 1 mL·min⁻¹ flow with mixtures of H₂O/0.045% TFA and acetonitrile/0.036% TFA and UV detection at 220 nm. Peptides were subsequently purified by preparative HPLC on a Waters Delta Prep 3000 system using a Phenomenex C18 (2) column (250 × 10 mm, 5 μm) eluted with H₂O/acetonitrile/0.1% TFA gradient mixtures and UV detection at 220 nm. Cyclization of peptides through disulfide bonds was carried out in 100 mM ammonium bicarbonate aqueous solutions with a pH adjusted to 10 by the addition of aqueous concentrated ammonia (32%). The final purity was greater than 95%. Peptides were characterized by amino acid analysis with a Beckman 6300 analyzer and by Matrix-Assisted, Laser Desorption/Ionization Time-of-Flight mass spectroscopy (MALDI-TOF) with a Bruker model Biflex III.

Lipid Vesicles. Unilamellar vesicles of POPG or POPA, alone or with the fluorescently labeled phospholipids—pyPG, pyPA, NBD-PE, or Rh-PE—were prepared by evaporation of a mixture of the lipids and probes in CHCl₃/CH₃OH (2:1, v/v). The dried film was hydrated for a final lipid concentration of 10 mM and then sonicated in a bath type sonicator (Lab Supplies, Hicksville, NY, model G112SPIT) until a clear dispersion was obtained (typically 2–4 min). Vesicle size was measured by dynamic light scattering with a Malvern II-C autosizer. Vesicles

have a mean diameter of 80 nm and a narrow size distribution (polydispersity <0.1).

Fluorescence Assays for Lipid Mixing. Fluorescence measurements were carried out at 23 °C in 10 mM Tris buffer at pH 8.0 on an AB-2 spectrofluorimeter (SLM-Aminco) with constant stirring. Typically, the slit widths were kept at 4 nm each and the sensitivity (PMT voltage) was adjusted to 1% for the Raman peak corresponding to the same excitation wavelength from the buffer blank. The exchange of lipid molecules between vesicles on the addition of the different peptides was assessed as described previously.^{11,12} Briefly, transfer of pyrene-labeled phospholipids as donor vesicles to an 100-fold excess of unlabeled phospholipid vesicles as acceptors was measured. Fluorescence emission was monitored at 395 nm (with excitation at 346 nm) corresponding to the monomer emission.

Peptide-mediated lipid mixing was also determined by RET from the NBD-PE donor to the Rh-PE acceptor. Covesicles containing 0.3 mol % of each of the probes were used to monitor (hemi)-fusion-induced dilution of the probes in excess unlabeled vesicles. Excitation was at 460 nm, and fluorescence emission from rhodamine was monitored at 592 nm. Vesicle-vesicle apposition without exchange of phospholipid was determined by RET, taking advantage of the fact that NBD-PE and Rh-PE do not exchange in the probe-dilution protocol described above. In this case, vesicles containing 0.6% NBD-PE or Rh-PE codispersed with suitable unlabeled lipids were mixed in a 1:1 ratio and titrated with peptides.

Tryptophan Fluorescence and Quenching Experiments. Tryptophan fluorescence spectra were recorded with an excitation wavelength of 285 nm over an emission range of 300–450 nm, with 4 nm slit widths. The peptide was added from a stock solution in water to a final concentration of 2.83 μ M, and vesicles were added to the desired lipid concentration. Titration of the peptide with vesicles was avoided due to the disruption of the vesicles that occurs at high peptide-to-lipid ratios. Spectra of vesicles with the same amount of the unlabeled peptide sP-B at the same lipid-to-peptide ratios were obtained and subtracted. Quenching of tryptophan fluorescence of sP-Bw by acrylamide was recorded at 330 nm (excitation 285 nm). Appropriate amounts of POPG or POPA vesicles were added to a solution of 5.65 μ M peptide, and aliquots of quencher were added with continuous stirring. Acrylamide was added from a 3.3 M stock solution in water to a final quencher concentration from 0 to 0.4 M. The Stern–Volmer quenching constants (K_{SV}) and the fraction of peptide accessible to acrylamide (f) were evaluated by curve fitting using the following equation:¹⁶

$$F_0/F - 1 = K_{SV}[Q]f/(1 + K_{SV}[Q](1 - f))$$

where F_0 and F are the fluorescence intensities in the absence and presence of quencher and $[Q]$ is the molar concentration of quencher.

Fluorescence Anisotropy. Steady-state tryptophan fluorescence anisotropy measurements were carried out in the same spectrofluorimeter with L-format polarizers. The excitation wavelength was set at 285 nm, and the emission, at 330 nm with excitation and emission slit widths at 4 nm. Titrations were carried out at 23 °C, adding aliquots of vesicles to a 2.83 μ M solution of sP-Bw in 10 mM Tris (pH 8.0). All solutions were stirred continuously during the measurements. The fluorescence anisotropy (r) was calculated automatically by the software provided with the instrument, according to

$$r = (I_{VV} - I_{VH})/(I_{VV} + 2I_{VH})$$

where I_{VV} and I_{VH} are the intensity of the emitted polarized light with the emission polarizer parallel or perpendicular to the excitation polarizer. Anisotropy values were automatically corrected for dependencies in the detection system (G-factor correction). Changes in anisotropy were represented as $(r - r_0)/r_0$, where r_0 and r are the anisotropy values before and after the addition of vesicles, respectively. All measurements were done in triplicate.

Fluorescence Resonance Energy Transfer (FRET) to Determine Peptide Binding. Binding of sP-Bw to vesicles of different compositions containing 2.5% NBD-PE was determined as the increase in the RET signal from Trp in the peptide to the labeled phospholipid in the interface at 535 nm (excitation 285 nm). Vesicles in buffer (20 μ M lipid) were titrated with peptide from a stock solution in water, and the relative change in fluorescence (δF) was obtained. δF is defined as $(F - F_0)/F_0$, where F_0 and F are the intensities without and with peptide, respectively. Due to the low lipid concentration used in this experiment, the contribution from light scattering is negligible.

Intermolecular FRET Measurements. The possibility of self-association of sP-B in solution or upon binding to the membrane was investigated using FRET from a donor population (Trp residue in sP-Bw) to an acceptor population (pyrene in the N-terminus of sP-Bpy, no Trp residues). Experiments were performed at an excitation of 295 nm, corresponding to Trp, and with the fluorescence emission of the acceptor (pyrene) monitored at 395 nm. The efficiency of energy transfer from Trp to pyrene (E) is defined by¹⁷

$$E = 1 - F_{DA}/F_D$$

where F_D is the fluorescence of the donor (sP-Bw) and F_{DA} is the fluorescence of the donor in the presence of the acceptor (sP-Bpy). Experiments were done in 10 mM Tris buffer at pH 8.0, by mixing acceptor (sP-Bpy) at a fixed concentration (7.57 μ M) with different amounts of donor (sP-Bw), followed by the addition of vesicles for a total peptide mole fraction of 1%. Results were analyzed assuming dimer formation, according to the following equation:¹⁸

$$F/F_0 - 1 = EX_d$$

where F and F_0 are the fluorescence of the acceptor bound to vesicles in the presence and absence of the donor, respectively, and X_d is the donor mole fraction. F_0 was obtained from control experiments where sP-Bw was substituted by the nonfluorescent sP-B parent peptide, maintaining the same concentrations of sP-Bpy and lipid. The time dependence of intermolecular Trp-pyrene FRET upon dimerization was monitored by manual mixing, using a small hole in the cover of the instrument to add the POPG vesicles to a mixture of donor and acceptor peptides and recording the change in the emission intensity of pyrene as a function of time with a resolution of 0.1 s.

Results and Discussion

Synthetic Px-B Analogue sP-B Forms Vesicle–Vesicle Contacts and Induces Selective Lipid Exchange. Transfer of phospholipids between vesicles induced by sP-B (structure in Figure 1b) was directly monitored as the change in the fluorescence intensity of pyrene-labeled phospholipids on dilution with unlabeled phospholipids. Emission from vesicles containing 30% pyrene phospholipid is dominated by the excimer band at 480 nm, and the intensity of the monomer band, at 395 nm, increases as the probe is diluted due to exchange with excess unlabeled vesicles in contact. As shown in Figure

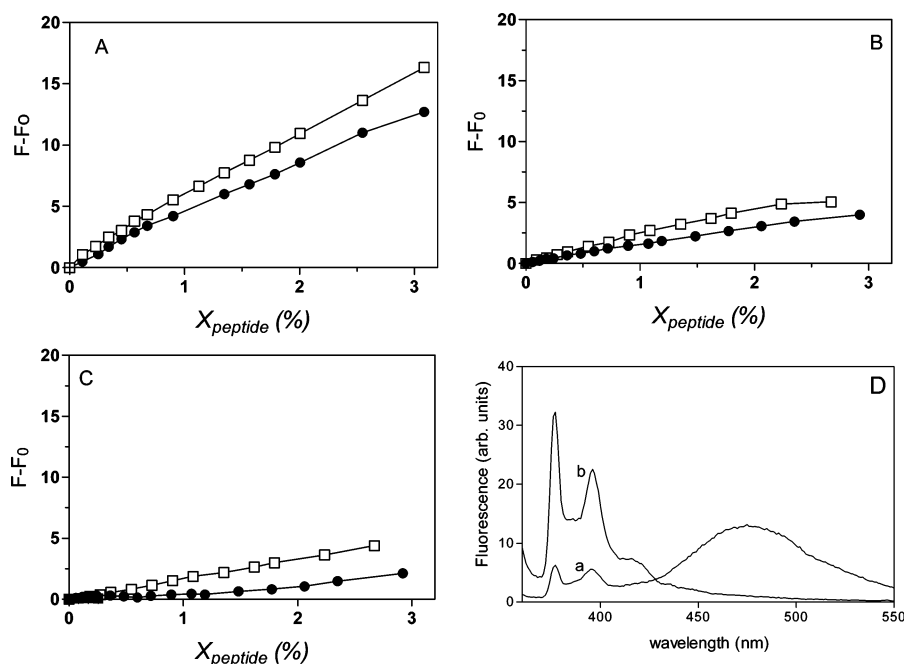


Figure 2. Fluorescence intensity of pyrene monomer as a function of peptide mole fraction in a mixture of vesicles: (A) PG/pyPG (7:3) with POPG; (B) PA/pyPA (7:3) with POPA; (C) PG/pyPA (7:3) with POPG. Peptides: PxB (open squares); sP-B (closed circles). Bulk lipid concentration $1.67 \mu\text{M}$ for py vesicles and $213.33 \mu\text{M}$ for unlabeled acceptor vesicles, in 10 mM Tris, pH 8.0. Excitation 346 nm, emission 395 nm. Part D shows representative spectra of (a) a mixture of pyPG and POPG and (b) the same with 4% sP-B.

2A, sP-B induces lipid exchange in a mixture of PG/pyPG (7:3) vesicles with 125-fold excess of PG vesicles, and the efficiency of transfer is comparable to that of PxB. Representative spectra of a mixture of labeled and unlabeled vesicles (1:100) alone and with sP-B are shown in Figure 2D. Lipid exchange is detected from very low mole fractions of sP-B in the membrane, even below 0.1%. This mole fraction corresponds to 8–9 peptide molecules per vesicle, considering that each unilamellar vesicle is formed by approximately 8000 lipid molecules. As already described for PxB, lipid exchange is very fast, complete in less than 5 s after peptide addition, and there is no time-dependent change in fluorescence, a clear indication of the absence of nonspecific fusion processes. We have previously demonstrated that PxB-induced vesicle–vesicle lipid exchange is specific¹² and that the specificity is related to the composition of the phospholipid headgroups. Monoanionic phospholipids such as PG or phosphatidylmethanol (PM) are rapidly exchanged through PxB contacts, independently of the phospholipid's fatty acid composition, whereas phospholipids with a dianionic headgroup such as PA, zwitterionic phosphatidylcholine (PC), as well as phospholipids with bulky labels in the headgroup, such as NBD or rhodamine groups, are excluded from the transfer. As shown in Figure 2B and C, the same specificity is observed for sP-B-mediated intervesicle exchange. Exchange of pyPA between PA vesicles in the presence of sP-B is very low (panel B). The most interesting observation is that pyPA is not exchanged even between vesicles of POPG (panel C), where the monoanionic lipid does exchange (see Figure 2A). This specificity indicated that sP-B forms intervesicle contacts with the same properties as those formed by the parent compound, PxB.

The specificity of lipid mixing was also monitored by a FRET assay using NBD and Rh labels covalently attached to the phospholipid headgroup (Figure 3). Coveicles containing 0.3% each of NBD-PE and Rh-PE in a matrix of PG or PA were mixed with a 50-fold excess of unlabeled vesicles and then titrated with increasing amounts of peptides. At low peptide

concentration, below 2 mol %, sP-B does not induce dilution of the probes in PG or PA vesicles (Figure 3A), indicating that the headgroup-labeled phospholipids are excluded from the contacts, a behavior already described for PxB-mediated vesicle–vesicle contacts.¹² In another set of experiments shown in Figure 3B, vesicles containing 0.6% NBD-PE were mixed with vesicles containing 0.6% Rh-PE, and in this case, an increase in energy transfer signal is observed in the presence of sP-B, with an increase in the intensity at 592 nm (rhodamine emission) and a corresponding decrease in the emission intensity from NBD (540 nm) (representative spectra are shown in Figure 3C). The increase in FRET is very similar for PG and PA vesicles. These results indicate that both monoanionic and dianionic vesicles form clusters in the presence of sP-B. In these clusters, NBD and Rh probes are in close proximity, resulting in measurable RET intensity (Figure 3B), even though the probes do not mix (Figure 3A). However, as shown in Figure 2, functional contacts are only formed in monoanionic vesicles. Taken together, the results in Figures 2 and 3 are consistent with vesicle aggregation and contact formation induced by sP-B, with a selectivity for the exchanged molecules related to the headgroup composition. These results are consistent with previously reported FRET experiments between PG vesicles containing pyPC and pyPG as donors and BODIPY-PC (4,4-difluoro-5-methyl-4-bora-3a,4a-diaza-s-indacene-3-dodecanoyl-3-dodecanoyl)-1-hexadecanoyl-*sn*-glycero-3-phosphocholine) as the acceptor.¹⁴ In this previous study, we demonstrated that sP-B-mediated vesicle–vesicle contacts were formed between PG vesicles and that lipid exchange was selective for PG, whereas PC was excluded.

Binding of sP-B to Lipid Vesicles Determined by Fluorescence Spectroscopy. Binding of sP-Bw to lipid vesicles results in changes in Trp emission spectra that depend on the vesicle composition, as illustrated in Figure 4 at 0.5 mol % peptide. Since tryptophan emission fluorescence depends on the environment, these changes can be used to study the penetration of the peptide into lipid bilayers.¹⁹ The spectrum of sP-Bw in

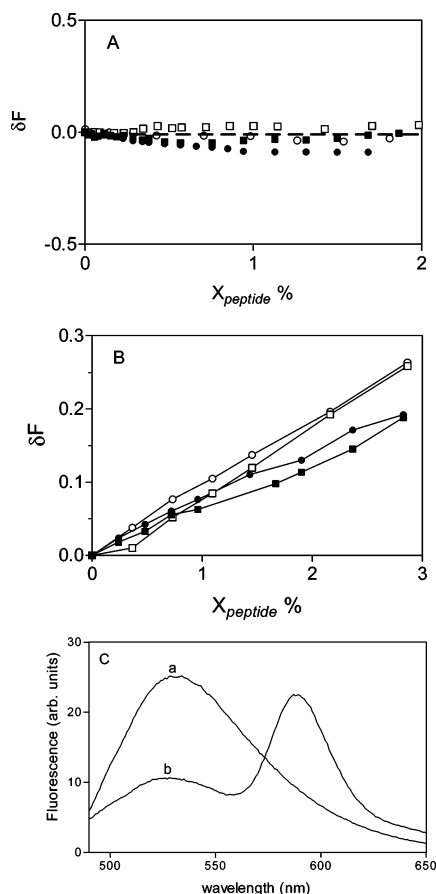


Figure 3. (A) Change in RET after mixing covesicles containing 0.3% NBD-PE and 0.3% Rh-PE (25 μM) with an excess of unlabeled vesicles (625 μM) in 10 mM Tris, upon addition of peptides. (B) Increase in RET intensity as a function of the mole fraction of peptide added to an equimolar mixture of vesicles containing 0.6% NBD-PE or Rh-PE; total lipid concentration 106.67 μM in 10 mM Tris. (C) Representative spectra of (a) a mixture of NBD and Rh-labeled POPG vesicles alone or (b) with 4% sP-B. Lipids: POPG (circles); POPA (squares). Peptides: Px-B (open symbols); sP-B (closed symbols). Excitation 460 nm, emission 592 nm.

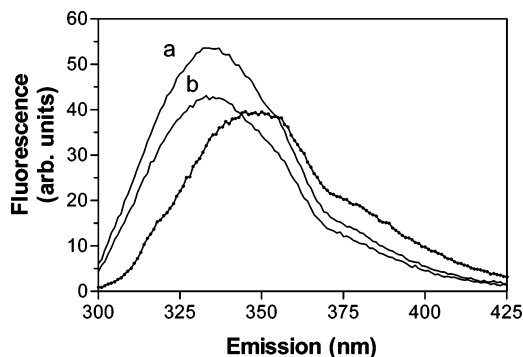


Figure 4. Tryptophan fluorescence emission spectra of sP-Bw in 10 mM Tris buffer (dotted line) or bound to vesicles of (a) POPG or (b) POPA. Excitation 285 nm. Peptide concentration 2.83 μM , lipid concentration 496.67 μM . Spectra were corrected by subtracting the corresponding spectra of sP-B (Trp-) obtained under the same conditions.

aqueous solution in the absence of vesicles has an emission maximum at 350 nm, indicating that the Trp residue is highly exposed to the aqueous environment.²⁰ The fluorescence properties of the peptide are markedly altered upon binding to anionic vesicles, as shown in the representative spectra of Figure 4 and

TABLE 1: Tryptophan Fluorescence Properties of sP-Bw

	λ_{em}^a (nm)	δF (340 nm)	r^a	K_{SV} (M^{-1})	f
buffer	350	0	0.0224	13.10	1.07
POPG	334	0.41	0.1808	2.92	1.05
POPA	334	0.12	0.1789	1.80	1.24

^a Peptide concentration 2.47 μM , peptide mole fraction 0.5%.

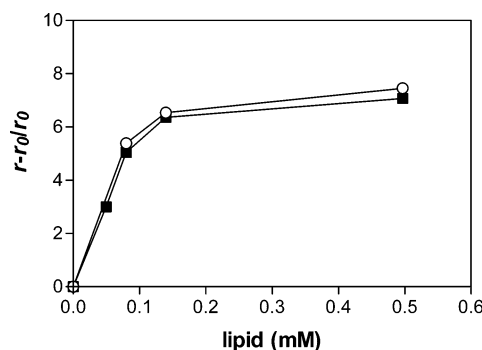


Figure 5. Fluorescence anisotropy change of sP-Bw as a function of lipid concentration: POPG (closed squares); POPA (open circles). The other conditions are the same as those in Figure 3.

summarized in Table 1. Interaction with monoanionic PG vesicles results in an important increase in tryptophan emission intensity, accompanied by a 16 nm blue shift in the position of the emission maximum. These changes indicate that the Trp residue is located in a more hydrophobic environment due to peptide transfer from the aqueous environment into the lipid environment. Binding to the dianionic PA interface also results in a shift of the emission maximum of 16 nm, but the magnitude of the change in emission intensity is very low. Changes in the peptide rotational freedom on binding were determined by measuring the anisotropy of the Trp residue; the values are summarized in Table 1. The anisotropy of sP-Bw in solution is low, $r_0 = 0.0224$, indicating a high mobility for Trp and therefore suggesting a disordered or random peptide conformation, which is expected due to the small size of the lipopeptide. Anisotropy changes for sP-Bw titrated with PG or PA vesicles are shown in Figure 5. Incorporation of sP-Bw in PG or PA vesicles results in similar changes in anisotropy, with a gradual increase that indicates that the Trp residue in the bound peptide is in a motionally restricted region.

Binding of sP-B to Vesicles Determined by FRET. The differences in Trp emission intensity of sP-Bw bound to PG versus PA vesicles (Figure 4) can be due to lower peptide binding to the dianionic vesicles or to a different form of the bound peptide depending on the charges at the interface. To distinguish these two possibilities, the binding of sP-B to vesicles containing 2.5% NBD-PE was determined by the increase of resonance energy transfer (RET) from the Trp donor of the peptide to the NBD acceptor at the interface. As shown in Figure 6, the RET intensity at 535 nm increases with the amount of peptide added, and the higher increases correspond to the PA vesicles. This indicates that sP-Bw binds to the anionic interfaces but that the tryptophan environment of bound sP-Bw depends on the lipid composition. In conjunction with the reported specificity for the phospholipid composition (Figures 2 and 3), these results suggest that binding is a necessary but not a sufficient condition for the formation of vesicle-vesicle contacts.

Quenching of sP-Bw by Acrylamide. An additional criterion for revealing the interaction of peptides with the lipid membrane is the analysis of the accessibility of Trp residues to acrylamide,

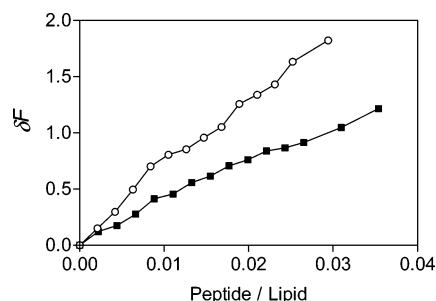


Figure 6. Change in FRET intensity at 535 nm (excitation at 285 nm) resulting from the addition of sP-Bw to vesicles containing 2.5% NBD-PE: POPG (closed squares); POPA (open circles). Lipid concentration 20 μ M.

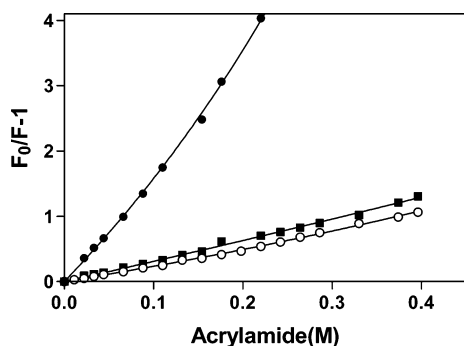


Figure 7. Stern–Volmer plots showing the tryptophan fluorescence quenching of sP-Bw (5.65 μ M) by acrylamide. Peptide in buffer (closed circles) or in the presence of vesicles of POPG (closed squares) or POPA (open circles). Fitting of the data to the model described in the Experimental Section is shown as a continuous line. Peptide mole fraction 0.5%. Titrations in 10 mM Tris buffer at pH 8.0 and 25 $^{\circ}$ C. Excitation 285 nm, emission 340 nm.

an efficient neutral collisional quencher of indole derivatives. In the lipid environment, the accessibility of the Trp residues to the aqueous quencher should be reduced. Typically, fully exposed Trp residues have Stern–Volmer quenching constants (K_{SV}) above 8 M^{-1} ,²¹ whereas K_{SV} for inaccessible Trp can be close to 0 M^{-1} .²² Figure 7 depicts the quenching efficiency of Trp emission of sP-Bw peptide by acrylamide both in solution and in the presence of vesicles at a peptide mole fraction of 0.5 mol %. The Stern–Volmer plots shown in Figure 7 are analyzed in terms of a two-state model of quencher accessible and inaccessible chromophore (see the Experimental Section), and the values of K_{SV} and the fraction of sP-Bw accessible to acrylamide (f) are summarized in Table 1.

In the absence of vesicles, sP-Bw has a K_{SV} value of about 13 M^{-1} ; similar or even higher values have been reported for other peptides in solution, such as fusogenic peptides from hepatitis A virus,²³ mellitin,²⁴ and cyclic antimicrobial hexapeptides.²⁵ All of the Trp residues of sP-B in solution are accessible to acrylamide ($f \sim 1$), in agreement with the fluorescence emission spectra. On the other hand, sP-Bw bound to anionic vesicles is ~ 7 -fold less accessible to acrylamide, indicating a higher degree of shielding (Table 1). Fitting of the data to the two-state model gives f values close to 1 independently of the vesicle composition (Table 1). This indicates that, at this high lipid-to-peptide ratio, all of the peptide is bound to the membrane, but Trp residues are partially shielded from the aqueous solvent due to insertion in the bilayer. In monoanionic POPG vesicles, K_{SV} values of 2.9 M^{-1} indicate a high degree of shielding. Binding to dianionic vesicles is accompanied by

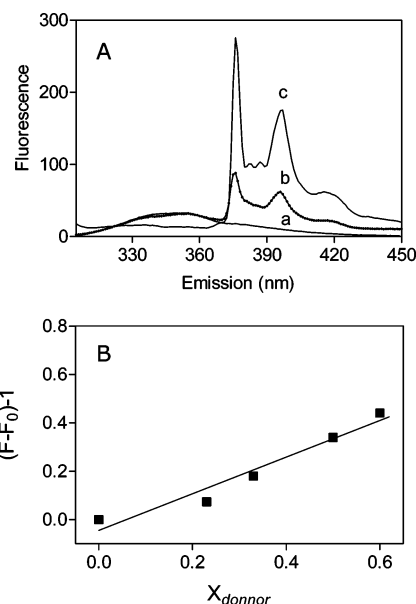


Figure 8. (A) Self-association of sP-B bound to vesicles of POPG detected by intermolecular Trp-pyrene FRET (excitation at 295 nm): (a) sP-Bw (21 nmol); (b) mixture of sP-w (21 nmol) and sP-Bpy (5.3 nmol); (c) same with POPG vesicles (total peptide mole fraction 1%). Experiments in 0.7 mL of 10 mM Tris, pH 8.0. (B) Fluorescence data for a series of experiments as in part A varying the donor concentration; the data were fitted by least-squares linear regression analysis according to the model described in the Experimental Section (continuous line).

a lower K_{SV} value (1.8 M^{-1}), indicating that Trp is even less accessible to the aqueous probe.

Intermolecular Fluorescence Resonance Energy Transfer. To determine peptide self-association upon membrane binding, Trp (donor)-to-pyrene (acceptor) intermolecular FRET was measured between sP-B tryptophan (sP-Bw)- and pyrene (sP-Bpy)-labeled analogues. Pyrene has an absorbance maximum at 340 nm, which is in the range of tryptophan emission. When these probes are in close proximity (the Förster distance for this pair is 27 Å), FRET is possible from tryptophan to pyrene, causing an increase in pyrene fluorescence. Intermolecular Trp-pyrene FRET is not detected on mixing of donor and acceptor peptides in the absence of vesicles (Figure 8A, spectra a and b). However, FRET takes place when the peptides are bound to POPG vesicles (spectrum c), suggesting that the peptide self-associates in the membrane. If a second aliquot of vesicles is added at the end, no further changes in the fluorescence emission of pyrene are seen (not shown but the same as spectrum c), indicating that all of the peptide was already bound to the vesicles. The increase in the fluorescence of sP-Bpy in the presence of varying amounts of donor species bound to PG vesicles is shown in Figure 8B. Each point in the figure corresponds to a separate experiment, and the total peptide mole fraction was kept constant at 0.5 mol %, representative of vesicle–vesicle contact formation without disruption of the vesicles. The results were analyzed following the theoretical model described for gramicidin²⁶ and colicin E1.¹⁸ According to this model, the fluorescence intensity of the acceptor is expected to increase linearly if dimers are formed (see the Experimental Section). The experimental data in Figure 8B are well fitted to this model ($r = 0.985$), thus suggesting that sP-B aggregates, probably dimers, are involved in vesicle–vesicle contact formation and lipid exchange. It is also interesting to note that sP-B molecules involved in vesicle–vesicle contacts are irreversibly bound, as already described for PxB in contacts.¹¹ For example, the fluorescence emission from sP-

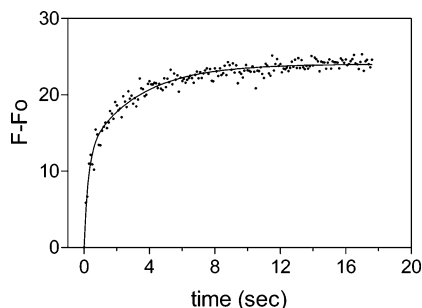


Figure 9. Kinetics of aggregation of sP-B monitored by intermolecular FRET. The data correspond to pyrene fluorescence intensity (395 nm) from the labeled sP-Bpy peptide (5.3 nmol) mixed with sP-Bw peptide (2.6 nmol) upon tryptophan excitation at 295 nm. Vesicles of POPG were added at time zero (peptide mole fraction 1 mol %), and the change in fluorescence was measured with a resolution of 0.1 s. The data were fitted with a double-exponential function, as described in the Results and Discussion section (continuous line).

Bpy increases 18% due to FRET from Trp when vesicles are added to an equimolar mixture of donor and acceptor peptides (Figure 8B), and no further increase in FRET is obtained if a second aliquot of sP-Bw is added next (not shown). This indicates that most of the pyrene peptide was already in the vesicle-vesicle contacts and that these contacts are irreversible.

The time dependence of intermolecular Trp-pyrene FRET upon binding to POPG vesicles was monitored, and the data were fitted with the equation

$$F - F_0 = A[1 - \exp(-k_1t)] + B[1 - \exp(-k_2t)]$$

where F is the fluorescence at time t , F_0 is the initial fluorescence at time zero, and k_1 and k_2 are the specific rate constants corresponding to two processes, with half-times of $0.69/k_1$ and $0.69/k_2$, respectively. The fits were judged to be good within 1%. In Figure 9, the kinetics of the dimerization of a mixture of sP-Bw and sP-Bpy (1:2) upon the addition of POPG vesicles is shown at a resolution of 0.1 s. Fitting of these data to the two-exponential equation (continuous line in Figure 9; $r = 0.98$) reveals that the progress curve can be resolved into two components: a fast process with a half-time of 0.18 s and a second process with a half-time of 2.20 s.

Conclusions

We have shown that sP-B, a synthetic analogue of PxB, binds irreversibly to anionic vesicles and induces the aggregation and formation of larger clusters at very low mole fractions of bound peptide. If the vesicles are formed by monoanionic phospholipids, sP-B forms molecular contacts and induces a selective lipid exchange in the same way as the parent peptide, PxB. In vesicles of dianionic phospholipids, sP-B does not induce the formation of functional contacts, although clusters of vesicles are formed. Intrinsic Trp fluorescence shows that sP-B binds

in a different form depending on the membrane composition, and FRET experiments are consistent with dimerization of the peptide in PG membranes, suggesting that dimers are responsible for the formation of functional vesicle-vesicle contacts. Since these contacts have been proposed as the molecular basis of the mechanism of action of PxB in Gram-negative bacteria,^{13,27,28} the data presented here show that sP-B is a promising molecule in the search for new antibiotics that act by the same mechanism as PxB.

Acknowledgment. This work was supported by a grant from the Ministerio de Ciencia y Tecnología-FEDER, SAF2002-01740 (to Y.C.), BQU2003-08174 (to F.R.), and Generalitat de Catalunya (Centre de Referència en Biotecnologia, CerBa).

References and Notes

- (1) Cassell, G. H.; Mekalanos, J. *JAMA, J. Am. Med. Assoc.* **2001**, *285*, 601–605.
- (2) Finlay, B. B.; Hancock, R. E. *Nat. Rev. Microbiol.* **2004**, *2*, 497–504.
- (3) Hancock, R. E.; Patrzykat, A. *Curr. Drug Targets: Infect. Disord.* **2002**, *2*, 79–83.
- (4) Brodgen, K. A. *Nat. Rev. Microbiol.* **2005**, *3*, 238–250.
- (5) Zasloff, M. *Nature* **2002**, *415*, 389–395.
- (6) Hancock, R. E. W.; Scott, M. G. *Proc. Natl. Acad. Sci. U.S.A.* **2000**, *97*, 8856–8861.
- (7) Gilliland, H. E.; Lyle, R. D. *J. Bacteriol.* **1979**, *138*, 839–845.
- (8) Denton, M.; Kerr, K. G. *Clin. Microbiol. Rev.* **1998**, *11*, 57–80.
- (9) Ouderkirk, J. P.; Nord, J. A.; Turett, G. S.; Kislak, J. W. *Antimicrob. Agents Chemother.* **2003**, *47*, 2659–2662.
- (10) Cajal, Y.; Berg, O. G.; Jain, M. K. *Biochem. Biophys. Res. Commun.* **1995**, *210*, 746–752.
- (11) Cajal, Y.; Rogers, J.; Berg, O. G.; Jain, M. K. *Biochemistry* **1996**, *35*, 299–308.
- (12) Cajal, Y.; Ghanta, J.; Easwaran, K.; Surolia, A.; Jain, M. K. *Biochemistry* **1996**, *35*, 5684–5695.
- (13) Oh, J. T.; Van Dyk, T. K.; Cajal, Y.; Dhurjati, P. S.; Sasser, M.; Jain, M. K. *Biochem. Biophys. Res. Commun.* **1998**, *246*, 619–623.
- (14) Clausell, A.; Rabanal, F.; García-Subirats, M.; Alsina, M. A.; Cajal, Y. *Luminescence* **2005**, *20*, 117–123.
- (15) Rabanal, F.; Tusell, J. M.; Sastre, L.; et al. *J. Pept. Sci.* **2002**, *8*, 578–588.
- (16) Talbot, J. C.; Thiaudiere, E.; Vincent, M.; Gally, J.; Siffert, O.; Dufourq, J. *Eur. Biophys. J.* **2001**, *147*–161.
- (17) Lakowicz, J. R. *Principles of fluorescence spectroscopy*; Plenum Press: New York, 1983; Chapter 10, pp 305–337.
- (18) Steer, B. A.; Merrill, R. *Biochemistry* **1997**, *36*, 3037–3046.
- (19) Galla, H. J.; Warncke, M.; Scheit, K. H. *Eur. Biophys. J.* **1985**, *12*, 211–216.
- (20) Burstein, E. A.; Vedenkina, N. S.; Ivkova, M. N. *Photochem. Photobiol.* **1973**, *18*, 263–279.
- (21) Wimley, W. C.; Creamer, T. P.; White, S. H. *Biochemistry* **1996**, *35*, 5109–5124.
- (22) Liu, L. P.; Deber, C. M. *Biochemistry* **1997**, *36*, 5476–5482.
- (23) Chávez, A.; Pujol, M.; Haro, I.; Alsina, M. A.; Cajal, Y. *Biopolymers* **2001**, *58*, 63–77.
- (24) Cajal, Y.; Jain, M. K. *Biochemistry* **1997**, *36*, 3882–3893.
- (25) Dathe, M.; Nikolenko, H.; Klose, J.; Bienert, M. *Biochemistry* **2004**, *43*, 9140–9150.
- (26) Veatch, W.; Stryer, L. *J. Mol. Biol.* **1977**, *113*, 89–102.
- (27) Oh, J. T.; Cajal, Y.; Dhurjati, P. S.; Van Dyk, T. K.; Jain, M. K. *Biochim. Biophys. Acta* **1998**, *1415*, 235–245.
- (28) Oh, J. T.; Cajal, Y.; Skowronska, E. M.; Belkin, S.; Chen, J.; Van Dyk, T. K.; Sasser, M.; Jain, M. K. *Biochim. Biophys. Acta* **2000**, *1463*, 43–54.